

Unsupervised Graph-based Learning Method for Sub-band Allocation in 6G Subnetworks

Daniel Abode^{1,2}, Ramoni Adeogun¹, Lou Salaün³, Renato Abreu², Thomas Jacobsen², Gilberto Berardinelli¹

¹*Department of Electronic Systems, Aalborg University, Denmark.*

²*Nokia, Aalborg, Denmark.*

³*Nokia Bell Labs, Massy, France*

Email: ^{1,2}{danieloa, ra, gb}@es.aau.dk, ²renato.abreu@nokia.com, ²thomas.jacobsen@nokia.com,

³lou.salaun@nokia-bell-labs.com

Abstract—In this paper, we present an unsupervised approach for frequency sub-band allocation in wireless networks using a graph-based learning method. We consider a scenario of dense deployment of subnetworks in the factory environment. The limited number of sub-bands must be optimally allocated to coordinate inter-subnetwork interference. Traditional iterative solutions may not scale to the large scale and density of sub-network deployment due to their execution overhead limitations. Hence, we consider a data-driven approach based on graph neural networks. We model the subnetwork deployment as an interference graph and propose an unsupervised learning approach to optimize the sub-band allocation using graph neural networks. This approach is inspired by the graph colouring heuristic and the Potts model. The numerical evaluation shows that the proposed method achieves close performance to the centralized greedy colouring sub-band allocation heuristic with lower computational time complexity. In addition, it incurs reduced signalling overhead compared to iterative optimization heuristics that require all the mutual interfering channel information. We further demonstrate that the method is robust to different network settings.

Index Terms—Sub-band allocation, interference coordination, graph neural networks, subnetworks, 6G.

I. INTRODUCTION

The densification of wireless networks is necessary to support the growing connectivity demand, a trend that will continue towards sixth generation (6G) [1]. The authors in [2] envisioned 6G to be a “network of networks”, where autonomous short-range low-power subnetworks inside entities such as vehicles, robots, industrial modules etc. can offload local communication within the entities from the central network. However, subnetwork deployments are expected to be extremely dense and large in scale in most use cases. For instance, in a factory scenario, numerous production modules and robots carrying subnetworks may be in proximity. The high density and large scale lead to significant inter-subnetwork interference, presenting a major limitation to the achievable spectral efficiency [3]. Consequently, efficient

methods including frequency allocation are being studied to mitigate the interference limitation [4]–[6].

Interference mitigation via frequency allocation typically involves dividing the available bandwidth into sub-bands, or frequency channels to be reused at different cells in the network. This essentially prevents adjacent cells from operating on the same sub-band or channel. Frequency reuse is crucial to balance the tradeoff between maximizing the cellular network’s ability to accommodate more users and mitigating interference [7]. However, the number of sub-bands is usually limited compared to the number of cells. Hence, optimally allocating the sub-bands results in a combinatorial optimization problem which is known to be NP-hard [7]. In traditional cellular architecture, where cell deployment is coordinated and static, optimized fixed frequency reuse patterns are generally efficient [7]. However, in subnetworks, wireless cells are installed inside entities including vehicles, humans and robots which are mobile. In this case, the fixed-frequency reuse pattern is insufficient. Consequently, various sub-optimal heuristics and data-driven solutions are being developed to cope with the dynamic nature of inter-subnetwork interference. In the literature, centralized schemes such as centralized graph colouring (CGC) [3] and sequential iterative sub-band allocation (SISA) [5] have been shown to achieve a better gain in spectral efficiency than distributed schemes.

In [5], the authors introduced SISA to address the issue of inter-subnetwork interference. They formulated an optimization problem to minimize the sum of the interference-to-signal ratio across all subnetworks. They developed a centralized solution that iteratively allocates sub-bands based on the channel information of the inter-subnetworks interference links and the intra-subnetwork desired links. However, the drawback of this method lies in the spectral cost associated with gathering the channel information of the mutual inter-subnetwork interference and the subsequent signalling of this information to the centralized agent responsible for executing the sub-band allocation algorithm. This cost increases quadratically with the number of subnetworks [6], hence the method is unsuitable for large-scale deployment.

Alternatively, the sub-band allocation can be formulated as a graph colouring problem as in [3], [8], [9], where Access Points (AP) or cells are represented as nodes in a graph and the

The work by Daniel Abode was supported by the Horizon 2020 research and innovation programme under the Marie Skłodowska-Curie grant agreement No. 956670. The work by Gilberto Berardinelli, Renato Abreu, Thomas Jacobsen, and Ramoni Adeogun was supported by the HORIZON-JU-SNS-2022-STREAM-B-01-03 6G-SHINE project (grant agreement No. 101095738). Ramoni Adeogun’s work was also partly supported by HORIZON-JU-SNS-2022-STREAM-B-01-02 project - CENTRIC (grant agreement No. 101096379)

edges model mutual interference. The graph is designed so that the chromatic number is either the same as the number of sub-bands or very close to it. The chromatic number of a graph is the number of colours required to colour the nodes of the graph such that no adjacent nodes have the same colour. The graph colouring problem defines the assignment of colours (sub-bands) to nodes (AP or cell) such that no nodes connected by an edge (i.e., adjacent nodes) are assigned the same colour [8]. Formulating sub-band allocation as a graph colouring problem is advantageous because wireless networks can be naturally represented as graphs. Additionally, graph colouring has been extensively studied, resulting in several heuristic solutions. The common solutions use a sub-optimal greedy colouring algorithm since exact solutions are typically exponential in complexity [10]. One significant benefit of modelling the sub-band allocation as graph colouring is the decrease in signalling cost. This is because the construction of the input graph only requires information about a small subset of the strongest interfering neighbours of each subnetwork, rather than the full channel information of both the desired and interfering links required in SISA.

In this paper, we propose a method inspired by the graph colouring heuristic. Our approach aims to reduce signalling costs while employing a data-driven approach for reduced runtime complexity. Recently, there has been a growing interest in using a data-driven approach to solve combinatorial optimization problems such as graph colouring [11], [12]. This is driven by the goal of reducing runtime costs, particularly for large-scale scenarios. We also consider an unsupervised data-driven approach to reduce training costs. Supervised learning approaches such as in [13] require the generation of large datasets including ground truths for training, which is complex to generate in practice. However, notable advances have been made in unsupervised learning approaches that do not require the complex procedure of generating ground truth using heuristics. Unsupervised methods have been shown to effectively solve combinatorial optimization problems using graph neural networks (GNN) [12]. This paper presents a novel unsupervised graph-based learning method for sub-band allocation. The approach incorporates a loss function based on the Potts model which penalizes the allocation of the same sub-band to adjacent nodes. This loss function does not depend on channel gain information. We employ a Gated Graph Neural Network (GGNN) as the graph-based learning model. It has been demonstrated to efficiently learn the graph structure for making inferences in sequential and combinatorial problems [14]. The GGNN is permutation-equivariant, scalable to changes in the size of the wireless network, and robust to different channel measurements. In addition, it can be executed in a centralized or decentralized manner.

Our major contributions are as follows;

- We represent the subnetworks deployment as an interference graph based on information on the strongest interfering neighbours of each subnetwork.
- We model the sub-band allocation as a node classification task and propose an unsupervised graph-based learning

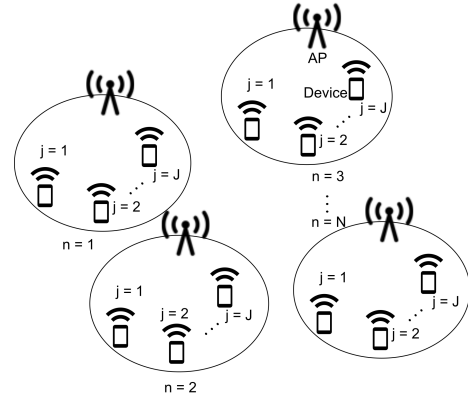


Fig. 1. Deployment of N subnetworks with J devices

approach inspired by the Potts model.

- We conduct extensive simulations to evaluate the performance and complexity of the approach compared to heuristic benchmarks. Furthermore, we evaluate the generalizability of the approach to different numbers of subnetworks, deployment density and channel models.

The rest of the paper is structured as follows. The next section presents the subnetwork system model and the problem formulation for sub-band allocation. In Section III, we describe the proposed GGNN algorithm followed by the performance evaluation and the simulation assumption in Section IV. Finally, we give some concluding remarks and future directions in Section V.

II. SYSTEM MODEL AND PROBLEM FORMULATION

A. Subnetworks System Model

We consider a network of $\mathcal{N} = \{1, 2, 3, \dots, N\}$ subnetworks which are densely and randomly deployed in an area as shown in Fig. 1 [3]. Each subnetwork consists of an AP that coordinates the communication of its $\mathcal{J} = \{1, 2, \dots, J\}$ connected devices. The subnetwork and devices are indexed with $n \in \mathcal{N}$ and $j \in \mathcal{J}$ respectively. We assume that the subnetworks operate over a synchronized time-frequency resource grid with the available bandwidth divided into K orthogonal sub-bands, where $K \ll N$. Hence, the K sub-bands are expected to be reused by multiple subnetworks, generating mutual interference. The sub-bands allocated to a subnetwork are further partitioned into orthogonal time-frequency slots so that each device in a subnetwork is allocated a dedicated time-frequency slot to avoid intra-subnetwork interference. We assume that each subnetwork can be allocated only one sub-band $k \in \{1, 2, \dots, K\}$, which is identified by a one-hot encoded vector $\theta_{\mathbf{n}} \in \mathbb{B}^K$. Hence, for the network of N subnetworks, we can define a sub-band selection matrix $\Theta \in \mathbb{B}^{K \times N}$, such that $\theta_{\mathbf{n}} = \Theta[:, n]$. The signal-to-interference noise ratio (SINR) of the uplink transmission between the j th device and the AP in subnetwork n occupying a channel slot in sub-band $\theta_{\mathbf{n}}$, with a channel gain, $\gamma_{j,n}$ and fixed transmit power, p_t can be written as

$$\Gamma_{j,n} = \frac{p_t |\gamma_{j,n}|^2}{\sum_{\substack{m=1 \\ m \neq n}}^N \mathbb{1}(\theta_n, \theta_m) p_t |\gamma_{j',m,n}|^2 + \sigma^2}, \quad (1)$$

$$\mathbb{1}(\theta_n, \theta_m) = \begin{cases} 1, & \text{if } \theta_n = \theta_m \\ 0, & \text{Otherwise,} \end{cases} \quad (2)$$

where $j' \in \mathcal{J}$ identifies the interfering device in subnetwork $m \in \mathcal{N}, m \neq n$ operating over the same time-frequency slot as device j in subnetwork n with the corresponding interfering channel gain, $\gamma_{j',m,n}$. σ^2 denotes the thermal noise power.

B. Interference Graph Model of Subnetworks

The subnetwork deployment can be represented as a graph $G(\mathcal{V}, \mathcal{E})$, where the set of nodes $\mathcal{V} = \{1, 2, \dots, N\}$ represent the subnetworks and the set of edges $\mathcal{E} = \{(n, m) : n, m \in \mathcal{V}\}$ represents potential inter-subnetwork interference. An edge exists if subnetwork n and subnetwork m are considered neighbouring subnetworks, i.e. $m \in \mathbb{N}(n)$ which can be based on different rules, where $\mathbb{N}(n)$ denotes a set of the neighbours of n . Foremost, the resulting interference graph must have a chromatic number of K . That is, it should be possible that all the nodes in the subnetwork interference graph can be allocated orthogonal sub-bands such that no adjacent nodes are allocated the same sub-band given a maximum of K sub-bands. One possible approximation to consider when building the subnetwork interference graph described in [3] is to connect each subnetwork to $K - 1$ strongest interfering neighbours. In this way, we consider a set \mathcal{M}_{I_n} which includes all the $K - 1$ strongest interfering subnetworks to subnetwork n . $G(\mathcal{V}, \mathcal{E})$ is built, such that;

$$\{\forall(n, m) | \mathcal{E}_{n,m} = 1 \text{ if } m \in \mathcal{M}_{I_n}, \text{ else } \mathcal{E}_{n,m} = 0\}, \quad (3)$$

C. Sub-band Allocation as a Node Classification Task

Given the subnetwork deployment interference graph $G(\mathcal{V}, \mathcal{E})$, the node $n \in \mathcal{V}$ is labelled by the sub-band selection θ_n . The optimization problem is to select θ_n, θ_m such that $\mathbb{1}(\theta_n, \theta_m) = 0$ if $m \in \mathbb{N}(n) \forall n$ which would intuitively minimize mutual inter-subnetwork interference. This optimization problem is similar to graph colouring [10]. According to [11], the Potts model on a graph $G(\mathcal{V}, \mathcal{E})$ defines the Hamiltonian of the interaction between adjacent nodes n, m with spin variables $\eta_n, \eta_m \in \{1, 2, \dots, K\}$ as

$$\mathcal{H}(\eta) = \sum_{(n,m) \in \mathcal{E}} \delta(\eta_n, \eta_m), \quad (4)$$

where, $\delta(\eta_n, \eta_m) = 0$ if $\eta_n \neq \eta_m$, which implies that the energy contribution of adjacent spins with different spin variables is zero, and positive otherwise. Essentially, if $G(\mathcal{V}, \mathcal{E})$ is K -colourable, to achieve a ground state energy of zero, the model penalizes adjacent spins that have the same spin variables. In relation, we can consider the sub-band allocation θ_n as a one-hot code for a spin variable η_n given the subnetwork interference graph. According to [12], the Hamiltonian can be reformulated in terms of the one-hot vector θ_n to derive the

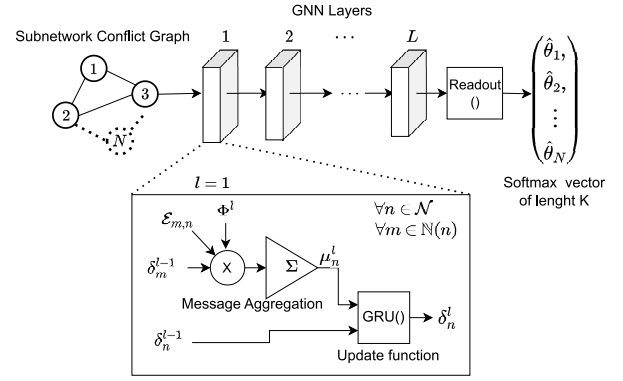


Fig. 2. Graph Neural Network Design

loss function [12]

$$\min_{\Theta} \Psi(\theta_n) = \sum_{(n,m) \in \mathcal{E}} \theta_n^T \cdot \theta_m. \quad (5)$$

This loss function would have a minimum value of zero if all the adjacent subnetworks are allocated orthogonal sub-bands, i.e. if $\theta_n \neq \theta_m \forall (n, m) \in \mathcal{E}$ corresponding to equation (4). For the unsupervised procedure that minimizes (5), we redefine the problem as a multi-class node classification, where a class is a sub-band. To enable a differentiable procedure, we replace the one-hot vector with a normalized smooth approximation of its class, $\theta_n \mapsto \hat{\theta}_n \in [0, 1]^K$. Hence,

$$\min_{\Theta} \Psi(\hat{\theta}_n) = \sum_{(n,m) \in \mathcal{E}} \hat{\theta}_n^T \cdot \hat{\theta}_m \quad (6)$$

The next section proposes the graph-driven model to learn $\hat{\theta}$ and describes the training procedure.

III. SUB-BAND ALLOCATION USING GRAPH NEURAL NETWORK

GNN is a family of neural network algorithms capable of learning from graph signals. As shown in Fig. 2, the GNN architecture consists of L layers. The propagation model in a GNN layer can be described using two functions, the message aggregation function and the update function. The message aggregation function is a permutation equivariant function that aggregates a pairwise exchange of embeddings between adjacent nodes. The update function generates a new embedding for the node from the aggregated messages. We adopt the GGNN model [14] for the message aggregation and update functions. The GGNN architecture utilizes a gated recurrent layer as the update function.

A. Gated Graph Neural Network Architecture

Given the interference graph of the subnetwork deployment $G(\mathcal{V}, \mathcal{E})$, the aggregated message for each node $n \in \mathcal{V}$ at layer $l \in \{1, 2, \dots, L\}$ as illustrated in Fig. 2 is given as;

$$\mu_n^l = \sum_{m \in \mathbb{N}(n)} \mathcal{E}_{m,n} \cdot \Phi^l \cdot \delta_m^{l-1}, \quad (7)$$

where Φ^l is the trainable feature transformation weight matrix of the message aggregation function, and δ_m^{l-1} denotes the pre-

vious node embedding of the neighbour. The update function is implemented using a gated recurrent unit (GRU), where the input is the aggregated message and the hidden state is the previous node embedding. So, the new embedding of node n at layer l is given as

$$\delta_n^l = \text{GRU}(\mu_n^l, \delta_n^{l-1}). \quad (8)$$

The GRU function consists of the reset gate r^l , update gate u^l and the new gates o^l which are define as

$$\begin{aligned} r^l &= \sigma(A_r^l \mu_n^l + a_r^l + B_r^l \delta_n^{l-1} + b_r^l), \\ u^l &= \sigma(A_u^l \mu_n^l + a_u^l + B_u^l \delta_n^{l-1} + b_u^l), \\ o^l &= \tau(A_o^l \mu_n^l + a_o^l + r^l \otimes (B_o^l \delta_n^{l-1} + b_o^l)), \end{aligned} \quad (9)$$

where $\sigma(\cdot)$ is a sigmoid activation function, $\tau(\cdot)$ is a hyperbolic tangent activation function. $A_r^l, B_r^l, A_u^l, B_u^l, A_o^l, B_o^l$ are trainable weights of the reset gate, update gate and new gate respectively, $a_r^l, b_r^l, a_u^l, b_u^l, a_o^l, b_o^l$ are their corresponding biases. The update function in (8) is then given as

$$\hat{\delta}_n^l = (1 - u^l) \otimes o^l + u^l \otimes \delta_n^{l-1}, \quad (10)$$

where \otimes denotes Hadamard product.

The trainable message aggregation weight allows the GGNN to learn the representation of the input graph structure while the update GRU allows the GGNN to learn the relationship between different intermediate internal embeddings in the L layers [14].

Finally, a readout function compresses the final node embedding after L GGNN layers into a normalized soft vector of size K , $\hat{\theta}_n$ as in

$$\hat{\theta}_n = \text{Softmax}(W \delta_n^L + b), \quad (11)$$

where W and b are the weights and biases of the readout function.

B. Training and Execution Procedure

We employed an unsupervised training algorithm which does not depend on any ground truth. The training graphs are generated using the interference graph model of the subnetworks. A mini-batch of graphs is propagated through the GGNN layers which execute (7), (8), and (11). The output $\hat{\theta}_n \forall n$ is passed to the loss function (6). By using mini-batch gradient descent, the $\hat{\theta}_n$ at training iteration t , $\hat{\theta}_n^t$ is updated as in

$$\hat{\theta}_n^t = \hat{\theta}_n^{t-1} - \vartheta \mathbb{E}_{\mathcal{B}} \nabla_{\hat{\theta}_n} \Psi(\hat{\theta}_n^{t-1}) \quad (12)$$

The training is terminated when $\mathbb{E}_{\mathcal{B}}(\Psi(\hat{\theta}_n^t) - \Psi(\hat{\theta}_n^{t-1})) < \epsilon$, where ϵ is the error tolerance, $\mathbb{E}_{\mathcal{B}}$ is the expectation over the batch of graph, and ϑ is the learning rate.

Since the input graphs have no attributes, all nodes are treated equally, hence the prediction depends on the structure of the graph which is learned during the message-passing procedure. The predicted sub-band for subnetwork n is given as $\text{argmax}(\hat{\theta}_n)$.

The trained model can be executed in a centralized or decentralized manner. For decentralized execution, each subnetwork

obtains a copy of the trained GGNN model and executes layer l to obtain embedding δ_n^l based on the message δ_m^{l-1} received from neighbouring subnetworks. Hence, such implementation would require L rounds of such message passing and the size of each message depends on the size of the embedding. This however would incur considerable signalling overhead and require synchronization between the subnetworks in executing each GGNN layer. On the other hand, centralized execution could be preferred if the subnetworks are within the coverage of a central network. In this case, the central network controller obtains the $K - 1$ neighbour identifiers for all subnetworks, builds the interference graph, executes the trained GGNN model, and signals the sub-band selection decision to the subnetworks.

IV. RESULTS AND DISCUSSION

In this section, we discuss the simulation assumption for the subnetwork deployment, the GGNN model selection and training parameters shown in table I, including brief descriptions of the benchmark algorithms. We compare the performance of the various benchmarks and our proposed approach in terms of the network spectral efficiency, execution complexity and generalizability. The spectral efficiency (SE) (bits/s/Hz) is approximated using Shannon capacity as $\text{SE}_{j,n} = \log_2(1 + \Gamma_{j,n})$.

A. Simulation Assumptions

1) Subnetwork Deployment

To evaluate the proposed method, we randomly deploy $N = 50$ subnetworks in a factory floor of size $40m \times 25m$ resulting in a density of 50000 subnetworks/km². We consider $K = 5$ sub-bands. To model the large-scale fading, we used the third generation partnership program (3GPP) technical report (TR) 38.901 Indoor Factory (InF) channel model [15] for the Dense-clutter Low-antenna (InF-DL) scenario and the associated model for the probability of non-line of sight (NLOS) and line of sight (LOS). The InF-DL scenario is appropriate since the subnetwork's AP and the devices are clutter-embedded. We consider full buffer uplink transmission. The transmission link path-loss, ρ is represented by the alpha-beta-gamma model [15]. The shadow fading s is modelled using the spatially correlated shadowing model used in [4]. The small-scale fading is Rayleigh distributed and complex-valued, denoted as $h \sim \mathcal{CN}(0, 1)$. Finally, the corresponding channel gain is then calculated as $\gamma = h \times \sqrt{10^{(\rho+s)/10}}$.

2) GGNN Model and Training Settings

The GGNN model is implemented with PyTorch Geometric and comprises $L = 10$ layers, with each layer having an output node embedding of size 64. The model is trained with 50000 graphs with a batch size of 64 graphs for 500 epochs, using the Adaptive Moment Estimation (ADAM) optimizer with an initial learning rate of 10^{-3} . The parameters of the training settings and the GGNN model in Table I were selected after conducting multiple experimental trials to determine the optimal configurations.

TABLE I
SIMULATION ASSUMPTION

Parameter	Value	Parameter	Value
Factory area	40m x 25m	Number of subnetworks, N	50
Subnetwork radius	2.5m	Number of devices per subnetwork	1
Minimum distance between APs	2.5m	Device to AP minimum distance	1m
InF-DL clutter density, clutter size	0.6, 2	Correlation distance	10m
Shadowing std (LOS, NLOS)	4dB, 7.2dB	Path loss exponent (LOS, NLOS)	2.15, 3.57
Transmit power	0 dBm	Number of sub-bands, K	5
Total bandwidth	20 MHz	Center frequency	28 GHz
Noise figure	10 dB	Number of GGNN layers	10
Size of embedding	64	Training epochs	500
Training data size	50000	Batch size	64
Initial learning rate	10^{-3}	Optimizer	ADAM

B. Benchmarks

To evaluate the performance of our proposed scheme in improving the network performance, we compare it with the following schemes;

- 1) Random Allocation (RA) - A distributed scheme where one sub-band is randomly selected from the available K options for each subnetwork.
- 2) Sequential Iterative Sub-band Allocation (SISA) - The sub-band selection sequential algorithm for subnetworks as detailed in [5] is a centralized iterative algorithm that minimizes the sum of the weighted interference.
- 3) Centralized Graph Coloring (CGC) - The approach described in [13] applies a greedy graph colouring heuristic for sub-band allocation in subnetworks. We applied this method to the same interference graph used for evaluating our proposed graph-based learning technique.

C. Network Performance Evaluation

Figures 3 and 4 show the empirical cumulative distribution function (CDF) of the sum SE and per-device SE, respectively, for the proposed scheme and the different benchmarks tested with 10000 network realizations. Given the interference graph, our proposed method outperforms random sub-band allocation by 20% in terms of achievable sum SE at the median. Below the median, GGNN achieves the same performance as CGC and lags behind SISA by 8%. However, note that SISA requires full channel gain information of all the mutual interfering links and desired links. Furthermore, GGNN can achieve a notable gain in per-device SE by up to 33% compared to Random subband allocation at the median as shown in Fig. 4.

D. Complexity Analysis

We analyzed the complexity of our proposed GGNN method and compared it with the benchmark algorithms, CGC and SISA in terms of the computational runtime and signalling requirement. Each algorithm is developed with Python frameworks and run on a Windows machine with an 11th Gen Intel(R) Core(TM) i7-11850H @ 2.50GHz processor and 32G memory. The result of the runtime analysis for different numbers of subnetworks, $N \in \{50, 60, \dots, 200\}$ in Fig. 5 is averaged over 10000 realizations. As shown in the figure, our GGNN method has a faster runtime, growing at a slower linear rate compared to the SISA and CGC. Hence, it would be more suitable for very dense networks with a large number of subnetworks or APs. While the runtime analysis is carried

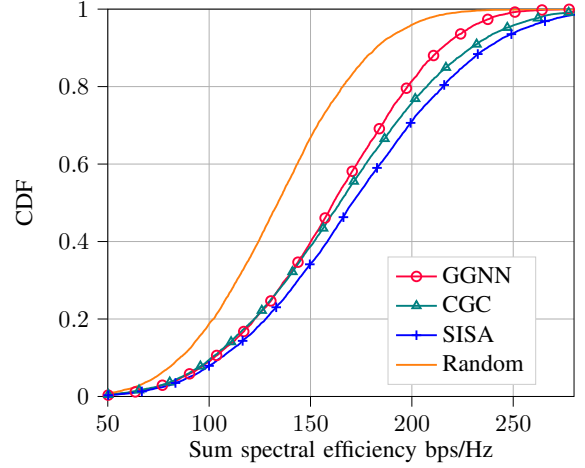


Fig. 3. Cumulative distribution function (CDF) of the sum spectral efficiency for 10000 test snapshots

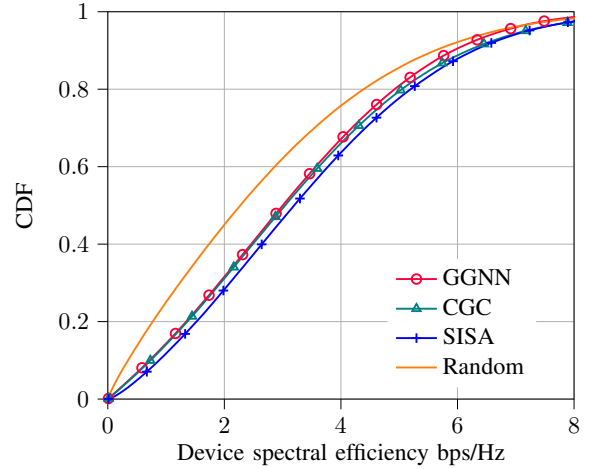


Fig. 4. Cumulative distribution function (CDF) of the per-device spectral efficiency for 10000 test snapshots

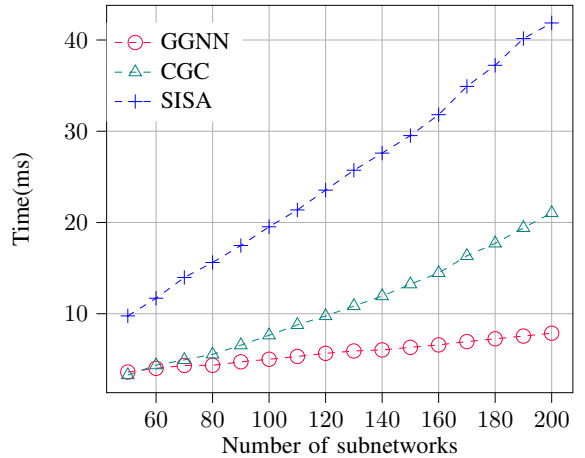


Fig. 5. Computational runtime for different number of subnetworks (ms) averaged over 10000 realizations

TABLE II

GENERALIZABILITY OF THE PROPOSED METHOD TO DIFFERENT NETWORK SETTINGS AND CHANNEL MODEL IN TERMS OF AVERAGE RATE (BPS/Hz)

		Test		
		Default	Scenario 1	Scenario 2
Train	Default	2.9445	2.8167	6.1154
	Scenario 1	2.9403	2.8124	6.1100
	Scenario 2	2.9298	2.7965	6.1238

out on a CPU, it is expected that the runtime for the GGNN method would further decrease on a GPU.

For the signalling overhead considering centralized implementation, the GGNN requires less information and therefore incurs fewer signalling resources than SISA. For example, N^2 signalling messages are required to be signalled to the central resource management entity from N subnetworks to execute the SISA algorithm; on the other hand, the GGNN method only requires $N(K-1)$ signalling messages, where $K \ll N$ in a large network. This further justifies the suitability of the proposed method for a large-scale deployment of subnetworks.

E. Generalizability

We analyze the ability of the proposed graph-based learning method to generalize to different network settings and channel models different from the training system model assumption as shown in table II. The default scenario is as presented in table I and we consider two different scenarios. Scenario 1 is a network consisting of 80 subnetworks deployed in a $50m \times 30m$ area, resulting in a 53300 subnetworks/ km^2 density, with the channel model based on 3GPP in-factory sparse clutter low antenna (InF-SL) model [15]. The NLOS path loss exponent, shadow fading standard deviation, clutter size and clutter density are 2.55, 5.7 dB, 10 and 0.35 respectively. Scenario 2 involves a less dense deployment of 20 subnetworks in $25m \times 25m$ area, i.e. 32000 subnetworks/ km^2 with path-loss modelled following the 3GPP model for inH-Office [15]. The NLOS path loss exponent, shadow fading standard deviation, and correlation distance are 3.83, 8.03 dB, and $6m$. We trained different GGNN models from training graphs for a given scenario and tested them on all three scenarios. As shown in table II, we observe that the average SE from testing with 10000 snapshots remain relatively the same for a test scenario, regardless of the training scenario. This shows that the trained model can generalize to different numbers of subnetworks, density and channel models. The robustness to different settings is due to the fact that the GGNN model learns based on the graph structure, which depends on the graph construction rule and not the distribution of the channel model. On the other hand, a more detailed evaluation may be required to determine if the method can adapt to a much larger difference in density between the training and testing scenarios. It is important to note that if the number of sub-bands changes, a new GGNN model would be needed, since the size of $\hat{\theta}$ in (11) corresponds to the number of available sub-bands.

V. CONCLUSION AND FUTURE WORK

This paper investigates an unsupervised graph-based learning approach to sub-band allocation for dense wireless subnetworks. The topology of the subnetwork is represented as a graph and the sub-band allocation is formulated as a node classification task parameterized by GGNN using a loss function inspired by the Potts model. We show that our approach offers comparable performance and requires lower runtime and signalling overhead than the centralized benchmark heuristics. We further show that the trained GGNN model is scalable, agnostic to the channel model and can be executed in a centralized or decentralized manner. Hence, the approach can be suitable for large-scale deployment of subnetworks. To better take advantage of the data-driven technique, our future work will consider more complex scenarios including traffic and mobility, where graph-based learning methods could outperform heuristics using the predictive ability of data-driven techniques.

REFERENCES

- [1] Z. Zhang *et al.*, “6G Wireless Networks: Vision, Requirements, Architecture, and Key Technologies,” *IEEE Vehicular Technology Magazine*, vol. 14, no. 3, pp. 28–41, 2019.
- [2] H. Viswanathan and P. E. Mogensen, “Communications in the 6G Era,” *IEEE Access*, vol. 8, pp. 57 063–57 074, 2020.
- [3] R. Adeogun, G. Berardinelli, I. Rodriguez, and P. Mogensen, “Distributed Dynamic Channel Allocation in 6G in-X Subnetworks for Industrial Automation,” in *2020 IEEE Globecom Workshops (GC Wkshps)*, 2020, pp. 1–6.
- [4] R. Adeogun and G. Berardinelli, “Distributed Channel Allocation for Mobile 6G Subnetworks via Multi-Agent Deep Q-Learning,” in *2023 IEEE WCNC*, 2023, pp. 1–6.
- [5] D. Li, S. R. Khosravirad, T. Tao, and P. Baracca, “Advanced Frequency Resource Allocation for Industrial Wireless Control in 6G subnetworks,” in *2023 IEEE WCNC*, 2023, pp. 1–6.
- [6] S. Bagherinejad, T. Jacobsen, N. K. Pratas, and R. O. Adeogun, “Comparative analysis of sub-band allocation algorithms in in-body subnetworks supporting xr applications,” in *2024 IEEE WCNC*, 2024, pp. 1–6.
- [7] R. Y. Chang, Z. Tao, J. Zhang, and C.-C. Kuo, “A Graph Approach to Dynamic Fractional Frequency Reuse (FFR) in Multi-Cell OFDMA Networks,” in *2009 IEEE International Conference on Communications*, 2009, pp. 1–6.
- [8] C. Zhao, X. Xu, Z. Gao, and L. Huang, “A coloring-based cluster resource allocation for ultra dense network,” in *2016 IEEE ICSPCC*, 2016, pp. 1–5.
- [9] M. Silard, P. Fabian, G. Z. Papadopoulos, and P. Savelli, “Frequency reuse in iab-based 5g networks using graph coloring methods,” in *2022 Global Information Infrastructure and Networking Symposium (GIIS)*, 2022, pp. 104–110.
- [10] A. Kosowski and K. Manuszewski, “Classical coloring of graphs,” 2008.
- [11] L. Zdeborová and F. Krzakala, “Phase transitions in the coloring of random graphs,” *Phys. Rev. E*, vol. 76, p. 031131, Sep 2007.
- [12] M. J. A. Schuetz, J. K. Brubaker, Z. Zhu, and H. G. Katzgraber, “Graph coloring with physics-inspired graph neural networks,” *Phys. Rev. Res.*, vol. 4, p. 043131, Nov 2022.
- [13] R. Adeogun, G. Berardinelli, and P. Mogensen, “Learning to Dynamically Allocate Radio Resources in Mobile 6G in-X Subnetworks,” in *2021 IEEE 32nd Annual International Symposium on Personal, Indoor and Mobile Radio Communications (PIMRC)*, 2021, pp. 959–965.
- [14] Y. Li, R. Zemel, M. Brockschmidt, and D. Tarlow, “Gated graph sequence neural networks,” in *Proceedings of ICLR’16*, April 2016.
- [15] 3GPP, “Study on channel model for frequencies from 0.5 to 100 GHz,” 3rd Generation Partnership Project (3GPP), Technical Report (TR) 38.901, 04 2022, version 17.0.0.